# University of Groningen

## Structure and Dynamics of the Lowest Triplet State in p-Benzoquinone. III. A Study of the n and π Spin-Density Distribution

Lichtenbelt, Jan H.; Wiersma, Douwe A.; Jonkman, Harry T.; Velde, Gerrit A. van der

Link to publication in University of Groningen/UMCG research database

# STRUCTURE AND DYNAMICS OF THE LOWEST TRIPLET STATE IN $p$-BENZOQUINONE.
# III. A STUDY OF THE n AND π SPIN-DENSITY DISTRIBUTION

Jan H. LICHTENBELT, Douwe A. WIERSMA

*Laboratory for Physical Chemistry, University of Groningen, Groningen, The Netherlands*

and

Harry T. JONKMAN [*] and Gerrit A. VAN DER VELDE [**]

*Laboratory for Theoretical Chemistry, University of Groningen, Groningen, The Netherlands*

The results of an ab-initio SCF calculation of the hyperfine coupling parameters in the n$p$* lowest triplet state of $p$-benzoquinone are reported and discussed. New results of a ring carbon-13 and oxygen-17 ENDOR study on the lowest triplet state of $p$-benzoquinone are also reported. Excellent agreement with experiment is obtained for the anisotropic hyperfine interaction constants which implies that the SCF description of the singly occupied orbitals is basically correct. The basic picture of the lowest triplet excited state spin-density distribution that is obtained from theory and experiment is, that the excited $p$-electron is delocalized over the molecule, while the n-electron is largely (≈75%) confined to the oxygen atoms. The effect of the delocalization of the n-electron however is clearly evident from the experiments.

## 1. Introduction

In the past couple of years there has been significant progress in the understanding of the spectroscopic properties of the lowest n$p$* states in $p$-benzoquinone (PBQ). Especially from the pioneering work of Trommsdorff [1] it became clear that the quinones are very special in the sense that their lowest optically accessible g and u n$p$* electronic states are only split by a few hundred wavenumbers. Moreover the lowest n$p$* states are quite isolated from higher excited states of the molecule. These features then make the $p$-benzoquinones unique candidates for a detailed study of the effect of pseudo Jahn-Teller coupling among near degenerate states.

The qualitative effect of such a near degeneracy is well understood [2] but a quantitative understanding

of the details of the optical spectra in the quinones has not been obtained yet.

In our laboratory we have made special study of the lowest n$p$* triplet state in PBQ and some of its isotopes.

The lowest triplet state of PBQ is attractive for a spectroscopic study as it shows sharp absorption and emission spectra and therefore the effect of electric [3] and magnetic [4] fields on these spectra can be analyzed in great detail. Also EPR and ENDOR spectra of this state of the molecule in mixed [5] and isotopically mixed [6,7] crystals may be obtained. Especially the ENDOR experiments give new information on the wavefunctions of the unpaired electrons which play a dominant role in the vibronic coupling process.

In part I of this series [6] we have reported on the spectroscopy of the lowest n$p$* triplet state in PBQ. In part II [7] the results of an EPR and proton-ENDOR investigation on this state were reported. In a recent paper [8] we reported the results of an ENDOR study on the carbonyl-carbon-13 hyperfine coupling in the same state. In the present paper (part III) we wish to report some new ENDOR data on the lowest triplet

---

[*] Present address: Department of Chemistry, University of Utah, Salt Lake City, Utah, USA.
[**] Present address: Control Data Service, Rijswijk (ZH), The Netherlands.
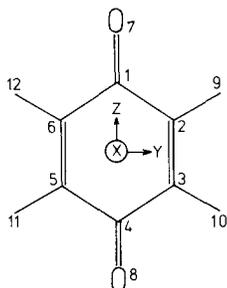
Fig. 1. Choice of axis system and numbering of the atoms in *p*-benzoquinone.

state of *p*-benzoquinone and to confront all the ENDOR data obtained so far [7,8] with the results of an ab-initio SCF calculation on PBQ.

It will be shown that the ab-initio molecular orbitals for the unpaired n and **p**-orbitals yield hyperfine interaction constants that compare very favourably with the experimentally observed ones. From this fact it is concluded that the SCF description of the singly occupied orbitals is basically correct.

The ab-initio results are further decomposed into atomic contributions which gives a detailed insight into the various contributions to the hyperfine coupling. From these calculations the limitations of a purely semi-empirical analysis of the ENDOR data also becomes very clear.

## 2. Computational details

The ab-initio SCF calculation of the hyperfine coupling constant in the lowest n**p**\* triplet state of PBQ were carried out with the program SYMOL [9] written by van der Velde. In the calculations the experimental geometry of the ground state of PBQ as reported by Trotter [10] was used and the atoms are numbered as shown in fig. 1. The basis set used consisted of six s and three p gaussian type orbitals (GTO's) on the C and O atoms, and three s GTO's on the H atoms.

The basis functions were contracted to a double zeta basis and the orbital exponents and the contraction coefficients used are identical to those previously employed by Jonkman et al. [11] in their calculation of the excitation energies of PBQ.

The main error in the present spin-density calcula-

tion probably stems from the neglect of all correlation (spin-polarization) effects. Especially the calculated spin-density of the s-orbitals on the carbonyl carbon and oxygen is zero, because both open shell orbitals have nodes on these atoms. For all other atoms both the isotropic and anisotropic hyperfine parameters are calculated. It should be noted that recently reported proton ENDOR [7] measurements on PBQ have shown that the molecule in the excited state is slightly distorted. A further complication, when comparing theory and experiments, arises from the fact that asymmetric isotopic substitution in PBQ is known to affect slightly the spin-density distribution in the lowest triplet state [6]. In the present calculation we have ignored these effects and assume that the molecule in the excited state preserves the full $D_{2h}$ symmetry.

## 3. Experimental

The isotopically mixed crystals of PBQ were grown in a Bridgeman furnace and cleaved or cut with a sharp razorblade in the desired direction. 7-$^{17}$O-PBQ-$h_4$ was prepared through exchange of the $^{16}$O-isotope with oxygen-17 enriched water (20%) in benzene, a procedure described by Becker et al. [12]. The enrichment of $^{17}$O in PBQ obtained, was found to be ca. 16% and mixed crystals with PBQ-$d_4$ were grown containing ca. 0.6 mol % of the $^{17}$O-PBQ isotope. The oxygen-17 enriched water was purchased from Stohler Isotopic Chemicals. 1, 2, 3, 5, 6-$^{13}$C$_5$-PBQ-$h_4$ was synethesized through oxidation of the corresponding aniline according to a procedure described by Willstätter and Dorogi [13].

In fact UL-$^{13}$C-analine (90 at%), also obtained from Stohler Isotopic Chemicals, was used in the synthesis. The ENDOR spectra of the oxidation product however clearly showed that the phosphorescing species in a PBQ-$d_4$ mixed crystal was the 1, 2, 3, 5, 6-$^{13}$C$_5$-PBQ-$h_4$ isotope. The UL-$^{13}$C-PBQ-$h_4$ species is either above or too close to the PBQ-$d_4$ host exciton band to act as a trap.

For further details of the ENDOR set-up we refer to previous reports of this laboratory on this subject [7,8].

Table 1
Fine-structure parameters and *g*-tensor principal values in the lowest triplet state of 1,2,3,5,6-$^{13}$C$_5$-PBQ-$h_4$ and 7-$^{17}$O-PBQ-$h_4$ as guests ($\approx$ 1 mol %) in PBQ-$d_4$ at 1.8 K as obtained from high field optically detected EPR measurements

|  | 1,2,3,5,6-$^{13}$C$_5$-PBQ-$h_4$ [a] | 7-$^{17}$O-PBQ-$h_4$ |
|---|---|---|
| *D* (MHz) | -2236 ($\pm$ 1.5) | $\approx$ -2051 |
| *E* (MHz) | 116 ($\pm$ 1.0) | $\approx$ 121 |
| $g_{xx}$ | 2.0053 ($\pm$ 0.0010) | |
| $g_{yy}$ | 2.0043 (($\pm$ 0.0010) | |
| $g_{zz}$ | 2.01002 ($\pm$ 0.00015) | $\approx$ 2.010 |

[a] Note that also in this PBQ isotope the fine-structure tensor is found to be ca. 5° rotated about the molecular *z* axes. In the analysis of the EPR data it is further assumed that the *g*- and fine-structure tensor spatially coincide.

## 4. Results

### 4.1. EPR and ENDOR data

Table 1 contains the fine-structure parameters and *g*-tensor principal values in the lowest triplet state of PBQ of those isotopically substituted species whereof we have obtained new ENDOR data. We will not comment on these parameters in this paper but it is interesting to nore that the *D* fine-structure parameter of

7-$^{17}$O-PBQ is virtually identical [7] to that of normal PBQ, while all other asymmetrically substituted PBQ's have significant different *D* fine-structure parameters [6-8]. The hyperfine interaction parameters of all isotopes measured so far are displayed in table 2. The proton and carbonyl-carbon-13 ENDOR data have been previously reported but the non-carbonyl-carbon-13 and oxygen-17 data are new. Table 2 shows that for 7-$^{17}$O-PBQ we have only been able to determine the absolute value of the *y*-element of the oxygen hyperfine inter-action constant.

The sign ambiguity in this case arises from the fact that this hyperfine element was obtained from high field EPR rather than ENDOR experiments. So far we have not been able to detect any fine structure on the EPR lines along the *x* and *z* magnetic field directions and therefore the *x* and *z* hyperfine elements are undeter-mined. We have also failed to detect oxygen ENDOR or CRENDOR transitions in 7-$^{17}$O-PBQ along any mag-netic field direction. Further note that in $^{13}$C$_5$-PBQ the ortho non-carbonyl-carbon atoms (C$_2$, C$_3$) have dif-ferent isotropic hyperfine interaction constants which shows that the spin-density distribution is sensitive to isotopic substitution.

### 4.2. Ab-initio SCF hyperfine interaction constants

From the SCF triplet state wavefunction we have

Table 2
Measured and calculated hyperfine interaction parameters of *p*-benzoquinone in its lowest n**p**\* triplet state. Note that all hyperfine interaction constants are given in MHz and that $j_z$ is the angle between the oxygen-oxygen direction and the *z*-axis of the (local) hyperfine tensor in the molecular plane

|  | Experimental | | | | | Ab-initio calculated [c] | | | | |
|---|---|---|---|---|---|---|---|---|---|---|
|  | $A_{xx}$ | $A_{yy}$ | $A_{zz}$ | $j_z$ | $A_{iso}$ | $A_{xx}$ | $A_{yy}$ | $A_{zz}$ | $j_z$ | $A_{iso}$ |
| C1 | 9.0 | -3.5 | -5.5 | 0.0° | -11.7 | 7.54 | -3.55 | -3.99 | 0.0° | 0.00 |
| C2 [a] | 2.8 | 2.0 | -4.7 | -26° | 17.4 | 2.93 | 1.55 | -4.48 | -25.0° | 25.47 |
| C3 | 2.8 | 2.0 | -4.7 | 28° | 19.3 | 2.93 | 1.55 | -4.48 | 25.0° | 25.47 |
| O7 | | |54.5| | | $\approx$ 0° | | 2.61 | -35.30 | 32.69 | 0.0° | 0.00 |
| H9,11 [b] | -3.1 | 4.7 | -1.6 | 17.9° | 9.6 | -3.09 | 4.47 | -1.38 | 14.5° | 6.38 |
| H10,12 | -3.1 | 4.7 | -1.6 | -12.4° | 9.6 | -3.09 | 4.47 | -1.38 | -14.5° | 6.38 |

[a] The absolute numbering of C-2 or -3 is not known.

[b] The proton-hyperfine interaction parameters of H$_{10,12}$ are slightly different from those previously reported [7]. This is due to the fact that in the previous analysis of the ENDOR data, the sign of one of the off diagonal hyperfine tensor elements was chosen wrongly. Full report on these data will be given in a future publication [31].

[c] In the calculations we have used the following conversion factors for $g_e\boldsymbol{b}_e g_n\boldsymbol{b}_n$; 79.063 MHz Å$^3$ for hydrogen, 19.890 MHz Å$^3$ for carbon and -10.716 MHz Å$^3$ for oxygen, where the *g*-values are assumed to be isotropic.

Tabel 3

Decomposition of the hyperfine interaction parameters into atomic contributions. Values in parentheses are interference contributions and contributions of symmetry related atoms are taken together. All hyperfine values are in MHz and $j_z$ is the angle between the oxygen-oxygen direction and the $z$ axis of the hyperfine tensor in the molecular plane

| | | $A_{xx}$ | $A_{yy}$ | $A_{zz}$ | $A_{zy}$ | $A_{iso}$ |
|---|---|---|---|---|---|---|
| (a) - C1 hyperfine interactions | | | | | | |
| C2, 3, 5, 6 | "1s" | - 0.01 ( 0.02) | 0.01 (-0.02) | 0.00 ( 0.00) | 0.00 ( 0.00) | 0.00 ( 0.00) [a] |
| H9,10,11,12 | 1s | - 0.01 ( 0.02) | 0.02 (-0.05) | -0.01 ( 0.03) | 0.00 ( 0.00) | 0.00 ( 0.00) |
| C2, 3, 5, 6 | "2s" | - 0.30 (-0.14) | 0.45 ( 0.29) | -0.15 (-0.15) | 0.00 ( 0.00) | 0.00 ( 0.00) [a] |
| C2, 3, 5, 6 | $2p_z$ | - 0.01 ( 0.06) | 0.02 (-0.15) | -0.01 ( 0.09) | 0.00 ( 0.00) | 0.00 ( 0.00) |
| O7, 8 | $2p_y$ | - 1.76 ( 0.38) | - 0.94 (-0.54) | 2.70 ( 0.16) | 0.00 ( 0.00) | 0.00 ( 0.00) |
| C1, 4 | $2p_y$ | - 1.18 (-0.13) | 2.35 ( 0.34) | -1.17 (-0.21) | 0.00 ( 0.00) | 0.00 ( 0.00) |
| C2, 3, 5, 6 | $2p_y$ | - 0.25 (-0.26) | 0.27 ( 0.43) | -0.01 (-0.17) | 0.00 ( 0.00) | 0.00 ( 0.00) |
| | | | | | | |
| All | n | - 3.58 | 2.48 | 1.11 | 0.00 | 0.00 |
| | | | | | | |
| O7, 8 | $2p_x$ | - 0.46 (-0.77) | - 0.96 ( 0.65) | 1.42 ( 0.13) | 0.00 ( 0.00) | 0.00 ( 0.00) |
| C1, 4 | $2p_x$ | 11.62 ( 0.10) | - 5.88 ( 0.26) | -5.73 (-0.35) | 0.00 ( 0.00) | 0.00 ( 0.00) |
| C2, 3, 5, 6 | $2p_x$ | - 0.10 ( 0.74) | 0.22 (-0.30) | -0.12 (-0.44) | 0.00 ( 0.00) | 0.00 ( 0.00) |
| | | | | | | |
| all | **p** | 11.12 | - 6.02 | -5.09 | 0.00 | 0.00 |
| | n + **p** | 7.54 | - 3.54 | -3.98 | 0.00 | 0.00 |
| | n | - 3.58 | 2.48 | 1.11 | 0.0° | 0.00 |
| diagonalised | **p** | 11.12 | - 6.02 | -5.09 | 0.0°(**j**$_z$) | 0.00 |
| | n + **p** | 7.54 | - 3.54 | -3.98 | 0.0° | 0.00 |
| | | | | | | |
| (b) - O7 hyperfine interactions | | | | | | |
| C2, 3, 5, 6 | "1s" | 0.00 ( 0.00) | 0.00 ( 0.00) | 0.00 ( 0.00) | 0.00 ( 0.00) | 0.00 ( 0.00) [a] |
| H9,10,11,12 | 1s | 0.00 ( 0.01) | 0.00 (-0.03) | 0.00 ( 0.02) | 0.00 ( 0.00) | 0.00 ( 0.00) |
| C2, 3, 5, 6 | "2s" | 0.05 (-0.11) | 0.00 ( 0.21) | -0.05 (-0.10) | 0.00 ( 0.00) | 0.00 ( 0.00) [a] |
| C2, 3, 5, 6 | $2p_z$ | 0.00 ( 0.04) | 0.00 (-0.10) | 0.00 ( 0.06) | 0.00 ( 0.00) | 0.00 ( 0.00) |
| O7, 8 | $2p_y$ | 23.12 (-0.17) | -46.19 ( 0.19) | 23.07 (-0.02) | 0.00 ( 0.00) | 0.00 ( 0.00) |
| C1, 4 | $2p_y$ | 0.03 (-0.05) | 0.02 ( 0.06) | -0.05 (-0.01) | 0.00 ( 0.00) | 0.00 ( 0.00) |
| C2, 3, 5, 6 | $2p_y$ | 0.03 (-0.04) | 0.00 ( 0.11) | -0.04 (-0.07) | 0.00 ( 0.00) | 0.00 ( 0.00) |
| | | | | | | |
| all | n | 22.92 | -45.74 | 22.82 | 0.00 | 0.00 |
| | | | | | | |
| O7, 8 | $2p_x$ | -22.05 ( 0.79) | 11.04 (-0.51) | 11.01 (-0.28) | 0.00 ( 0.00) | 0.00 ( 0.00) |
| C1, 4 | $2p_x$ | 0.07 ( 0.74) | 0.31 (-0.42) | -0.38 (-0.32) | 0.00 ( 0.00) | 0.00 ( 0.00) |
| C2, 3, 5, 6 | $2p_x$ | 0.05 ( 0.09) | 0.02 ( 0.01) | -0.07 (-0.10) | 0.00 ( 0.00) | 0.00 ( 0.00) |
| | | | | | | |
| all | **p** | -20.31 | 10.45 | 9.87 | 0.00 | 0.00 |
| | n + **p** | 2.61 | -35.29 | 32.69 | 0.00 | 0.00 |
| | | | | | | **j**$_z$ |
| | n | 22.92 | -45.74 | 22.82 | 0.0° | 0.00 |
| diagonalised | **p** | -20.31 | 10.45 | 9.87 | 0.0°(**j**$_z$) | 0.00 |
| | n + **p** | 2.61 | -35.29 | 32.69 | 0.0° | 0.00 |

Table 3 (continued)

|  |  | $A_{xx}$ | $A_{yy}$ | $A_{zz}$ | $A_{zy}$ | $A_{iso}$ |
|---|---|---|---|---|---|---|
| (c) C2 hyperfine interactions | | | | | | |
| C2, 3, 5, 6 | "1s" | -0.01 ( 0.00) | 0.00 ( 0.00) | 0.02 ( 0.00) | 0.00 ( 0.03) | 37.87 (-6.81) [a] |
| H9,10,11,12 | 1s | -0.04 (-0.04) | 0.04 ( 0.11) | 0.00 (-0.07) | 0.03 ( 0.03) | 0.01 ( 0.53) |
| C2, 3, 5, 6 | "2s" | -0.04 ( 0.05) | 0.00 (-0.09) | 0.04 ( 0.04) | 0.03 (-0.45) | 2.01 (-9.16) [a] |
| C2, 3, 5, 6 | $2p_z$ | -0.09 (-0.05) | -0.09 (-0.03) | 0.18 ( 0.07) | 0.00 (-0.52) | 0.03 ( 0.85) |
| O7, 8 | $2p_y$ | -0.40 ( 0.07) | -0.14 ( 0.00) | 0.54 (-0.07) | -0.29 ( 0.08) | 0.00 ( 0.03) |
| C1, 4 | $2p_y$ | -0.05 (-0.08) | 0.04 ( 0.09) | 0.01 (-0.02) | -0.06 (-0.09) | 0.00 (-0.05) |
| C2, 3, 5, 6 | $2p_y$ | -1.57 (-0.10) | 2.98 ( 0.16) | -1.41 (-0.06) | 0.05 (-0.77) | 0.00 ( 0.16) |
| all | n | -2.40 | 3.06 | -0.66 | 1.89 | 25.47 |
| O7, 8 | $2p_x$ | -0.18 ( 0.07) | -0.06 ( 0.00) | 0.24 (-0.07) | -0.16 ( 0.08) | 0.00 ( 0.00) |
| C1,4 | $2p_x$ | -0.22 ( 0.31) | 0.24 (-0.10) | -0.02 (-0.21) | -0.27 ( 0.00) | 0.00 ( 0.00) |
| C2, 3, 5, 6 | $2p_x$ | 5.04 ( 0.26) | -2.58 (-0.09) | -2.46 (-0.17) | 0.02 (-0.05) | 0.00 ( 0.00) |
| all | **p** | 5.29 | -2.60 | -2.69 | - 0.38 | 0.00 |
|  | n + **p** | 2.88 | 0.46 | -3.35 | 1.51 | 25.47 |
|  |  |  |  |  | $j_z$ | |
| diagonalised | n | -2.36 | 3.88 | -1.52 | -22.8° | 25.47 |
|  | **p** | 5.29 | -2.26 | -3.03 | -41.5° ($j_z$) | 0.00 |
|  | n + **p** | 2.93 | 1.55 | -4.48 | -25.0° | 25.47 |
| (d) - H9 hyperfine interactions | | | | | | |
| C2, 3, 5, 6 | "1s" | -0.07 ( 0.05) | 0.08 (-0.08) | -0.01 ( 0.02) | 0.09 (-0.05) | 0.00 ( 0.00) [a] |
| H9,10,11,12 | 1s | -0.01 (-0.02) | 0.00 (-0.17) | 0.01 ( 0.19) | 0.00 ( 0.10) | 3.82 ( 1.12) |
| C2, 3, 5, 6 | "2s" | -0.86 ( 0.70) | 1.38 (-0.59) | -0.52 (-0.11) | 0.89 (-1.03) | 1.45 (-4.48) [a] |
| C2, 3, 5, 6 | $2p_z$ | -0.02 ( 0.04) | 0.00 (-0.14) | 0.02 ( 0.11) | 0.00 (-0.04) | 0.07 ( 0.59) |
| O7, 8 | $2p_y$ | -1.12 ( 0.11) | 0.84 (-0.17) | 0.29 (+0.06) | -1.11 ( 0.06) | 0.00 ( 0.01) |
| C1, 4 | $2p_y$ | -0.06 (-0.04) | 0.10 ( 0.08) | -0.04 (-0.04) | 0.00 ( 0.04) | 0.00 ( 0.00) |
| C2, 3, 5, 6 | $2p_y$ | -0.97 ( 0.24) | 0.60 (-0.24) | 0.37 ( 0.00) | 1.59 (-0.50) | 2.28 ( 1.54) |
| all | n | -2.04 | 1.69 | 0.35 | 0.07 | 6.38 |
| O7, 8 | $2p_x$ | -0.50 ( 0.17) | 0.43 (-0.23) | 0.07 ( 0.06) | -0.47 ( 0.12) | 0.00 ( 0.00) |
| C1, 4 | $2p_x$ | -0.48 ( 0.01) | 0.87 ( 0.17) | -0.38 (-0.19) | 0.05 ( 0.23) | 0.00 ( 0.00) |
| C2, 3, 5, 6 | $2p_x$ | -0.15 (-0.10) | 0.85 ( 0.32) | -0.70 (-0.22) | 1.26 ( 0.16) | 0.00 ( 0.00) |
| all | **p** | -1.05 | 2.41 | -1.36 | 1.35 | 0.00 |
|  | n + **p** | -3.09 | 4.10 | -1.01 | 1.42 | 6.38 |
|  |  |  |  |  | $j_z$ | |
| diagonalised | n | -2.04 | 1.70 | 0.35 | 2.8° | 6.38 |
|  | **p** | -1.05 | 2.85 | -1.80 | 17.8° ($j_z$) | 0.00 |
|  | n + **p** | -3.09 | 4.47 | -1.38 | 14.5° | 6.38 |

[a] In the SCF wavefunction the carbon "2s" orbital contains only the "outer" part of the atomic carbon 2s orbital. For computational convenience the "inner" part is joined to the atomic 1s orbital to form the "1s" carbon SCF orbital.

calculated the isotropic and anisotropic hyperfine interaction constants and the results are also given in table 2. The table shows that the overall agreement, especially in the case of the anisotropic hyperfine interaction constants ($A_{aniso}$), between theory and experiment is very good. The calculation of the orientation of the principal axes of the hyperfine tensors is also in good agreement with experiment.

In order to be able to give more physical insight into the "meaning" of the results of the theoretical calculation we have unravelled the anisotropic hyperfine elements into atomic contributions. The results of this decomposition are gathered in table 3, which will form the basis for the following discussion.

A first conclusion we draw, from a look at table 3 is, that interference contributions (the sum of all atomic non-diagonal hyperfine interaction terms) to $A_{aniso}$, which in table 3 are within parentheses, are not negligible. In a McConnel-Strathdee [14] and point-dipole [15] calculation of the anisotropic hyperfine interaction constants these terms are not fully taken into account.

A second interesting conclusion is, that in a molecule of the size of PBQ for a calculation of the anisotropic hyperfine interaction constants, the *complete* unpaired electron density distribution has to be taken into account. This, of course, makes a purely semi-empirical determination of the excited state spin-density distribution extremely difficult.

We now proceed by discussing in greater detail, per atom, the highlights of table 3.

## 5. Discussion of the results

### 5.1. The carbonyl-carbon atom

Table 3a shows that the main contribution to $A_{aniso}$, as expected [8], is due to $2p_x(\boldsymbol{p})$ density at carbon itself. From a net population analysis (vide infra) it follows that the net $\boldsymbol{p}$-"spin-density" residing at this carbon atom is 0.156. We then calculate [†] a value of 150 MHz for the carbon-13 hyperfine interaction constant per unit $\boldsymbol{p}$ spin-density. This number is

---

[†]  In *all* calculations the normalization condition $\Sigma_i r_i^n + \Sigma_j r_j^p = 1$ is used, note however that in table 4 the n and $\boldsymbol{p}$ "spin-densities" individually are normalized ($\Sigma_i r_i^n = \Sigma_j r_j^p = 1$).

in good agreement with the value of 156 MHz reported by Adam and Weissman [16] and some 15% higher than the value reported by Smith et al. [17]. This latter value was recently used by us in a preliminary analysis of the carbon-13 ENDOR data [8].

Table 3a further shows that the contribution of the $2p_y(n)$ spin-density is far from negligible. Especially the contribution of the n spin-density residing at oxygen and carbon itself is shown to be important. Table 3a also shows that the contributions of the n and $\boldsymbol{p}$ spin-density to $A_{aniso}$ are indeed of opposite sign. This confirms one of our previous assumptions made in the semi-empirical analysis of the carbon-13 ENDOR data [8].

The isotropic hyperfine interaction constant is calculated to be zero. Its finite values (-11.7 MHz) therefore must be due to mixing with excited configurations in which open $a_g$ and $b_{1u}$ orbitals are occupied. Semi-empirically we can calculate $A^p_{iso}$ using the relation derived by Broze and Luz [18,19] for the carbon-13 isotropic hyperfine coupling. They obtain the following relation:

$$A^p_{iso}(C_1) = 145.9 \ \boldsymbol{r}^p_{C_1} - 38.9 \ (\boldsymbol{r}^p_{C_2} + \boldsymbol{r}^p_{C_6}) - 68.0 \ \boldsymbol{r}^p_{O_7} \text{ MHz.}$$

For the n-contribution the following relation then seems plausible:

$$A^n_{iso} (C_1) = -68.0 \ \boldsymbol{r}^n_{O_7} \text{ MHz.}$$

For the lowest triplet state in PBQ we then calculate, using the gross atomic population (GAP) spin-density of table 4 (vide infra)

$$A_{iso}^{n+p}(C_1) = -9.5 \text{ MHz,}$$

which is in reasonable agreement with the experimental value. The carbon-13 isotropic hyperfine coupling thus is dominated by polarization effects mainly of the n spin-density at oxygen.

### 5.2. The oxygen atom

Table 3b clearly shows that the oxygen hyperfine interaction parameters are almost exclusively due to n and $\boldsymbol{p}$ spin-density residing at the oxygen atom itself. The implication of this result is that measurement of these hyperfine parameters combined with knowledge of the oxygen atomic hyperfine interaction constant gives a precise determination of the $2p_x(\boldsymbol{p})$ and $2p_y(n)$ density at oxygen.

Our measurements of the total (isotropic plus anisotropic) hyperfine interaction constant $|A_{yy} + A_{iso}|$ suggests that $A_{iso} \approx -19.2$ MHz. The alternative choice of $A_{iso} \approx 89.8$ MHz is rejected as this would have certainly led to an observable hyperfine pattern for the magnetic field along the $x$ and $z$ molecular axes. The SCF calculation thus predicts hyperfine splittings of -16.6 and 13.5 MHz of the EPR transitions along the $x$ and $z$ molecular directions. Using the calculated n net atomic population of 0.394 at oxygen (vide infra) we calculate for the oxygen atomic interaction constant -235 MHz.

Morton [20] has calculated a value of -288 MHz for this constant but from the EPR measurements by Wong and Lunsford [21] on the $^{17}O^-$ ion this constant is found to be -231 MHz, in good agreement with our calculation. We further note that from the **p** net atomic population density this constant is calculated to be -200 MHz. This result shows that one cannot expect atomic hyperfine interaction constants to be identical for **p** and n electrons. This fact introduces an extra uncertainty in a semi-empirical analysis of hyperfine interaction constants.

### 5.3. The non-carbonyl-carbon atom

The dominant contribution to $A_{aniso}$ in this case arises from the $2p_x$ and $2p_y$ spin-density residing at the ring-carbon itself. The interference contributions however, especially from the unpaired n-density distribution, are not negligible. Table 3d further shows that the $zz$ element of the hydrogen atom hyperfine tensor is almost exclusively determined by the **p** density at the neighbouring carbon atom. Using the experimentally obtained value $A_{zz} = -1.6$ MHz we then calculate [19,22] for the **p** density at $C_2$, $\boldsymbol{r}^{p}_{C2} = 0.09$ which is in good agreement with the GAP spin-density of table 4. We have also analyzed the contributions of the different atomic orbitals to the isotropic hyperfine interaction constant of the ring-carbon atom. Table 3c shows that this constant is mainly determined by the unpaired spin-density in the s-orbitals of carbon. Interference effects in this case are also found to be very important. In a semi-empirical treatment of the isotropic hyperfine coupling we would have assumed that only the carbon 2s spin-density is responsible for $A^{n}_{iso}$.

The **p**-contribution to the isotropic hyperfine interaction can be calculated using the semi-empirical relation derived by Karplus and Fraenkel [23] :

$$A^{p}_{iso}(C_2) = 99.7 \; \boldsymbol{r}^{p}_{C_2} - 38.9 \; (\boldsymbol{r}^{p}_{C_1} + \boldsymbol{r}^{p}_{C_3})\text{MHz}.$$

Using the GAP spin-density of table 4 we calculate $A^{p}_{iso}(C_2) = -0.4$ MHz. We then "find", using the mean experimental value of $A_{iso}$ ($C_2,C_3$) of 18.3 MHz, for $A^{n}_{iso}$: $18.3 + 0.4 = 18.7$ MHz. For unit spin-density in a 2s carbon orbital the isotropic hyperfine splitting is known to be 3342 MHz [23]. We then calculate for the 2s spin-density of carbon (2) $\boldsymbol{r}^{n}_{C2} = 0.011$ which compares very nicely with the GAP spin-density displayed in table 4.

### 5.4. The hydrogen atom

Table 3d shows that there are numerous contributions to the anisotropic hyperfine coupling tensor of hydrogen. It therefore seems virtually impossible to calculate these tensor elements semi-empirically with any accuracy. The excellent agreement between the measured and calculated anisotropic hyperfine parameters of this atom further supports the idea that the SCF description of the singly occupied **p** and n-orbitals is basically correct.

We have also decomposed the hydrogen isotropic hyperfine coupling into atomic contributions and the results are also given in table 3d. Note that the interference contribution from the carbon 2s orbital gives the largest contribution to the isotropic hyperfine coupling. In a previous semi-empirical treatment of the proton ENDOR [7] , we assumed only the 1s spin-density at hydrogen itself to be responsible for the observed isotropic hyperfine coupling constant. In that calculation we ignored the contributions from other atoms and table 3d shows that this is clearly not warranted. The previous calculated 1s density at hydrogen thus must be considered an upper limit.

Further note that the experimentally measured value of the proton hyperfine coupling parameter also contains a contribution of polarization due to the unpaired **p** density. Taking this into account we calculate for $A^{n}_{iso} = 12.7$ MHz which is twice as large as the value of 6.39 MHz, obtained from an ab-initio calculation. This large discrepancy is mainly due to the fact that the wavefunction we use is known [24] to give a poor description near the nucleus.

Table 4
Gross (GAP) and net (NAP) atomic population densities as calculated from the ab-initio SCF wavefunction of the lowest n**p**\* triplet state in *p*-benzoquinone

|  |  | GAP | NAP |
|---|---|---|---|
| C2, 3, 5, 6 | "1s" | < 0.001 | 0.004 |
| H9,10,11,12 | 1s | 0.007 | 0.006 |
| C2, 3, 5, 6 | "2s" | 0.012 | 0.046 |
| C2, 3, 5, 6 | $2p_z$ | 0.001 | 0.002 |
| O7, 8 | $2p_y$ | 0.370 | 0.394 |
| C1, 4 | $2p_y$ | 0.016 | 0.012 |
| C2, 3, 5, 6 | $2p_y$ | 0.036 | 0.033 |
|  | Σ | 1.000 | 1.176 |
|  |  |  |  |
| O7, 8 | $2p_x$ | 0.153 | 0.220 |
| C1, 4 | $2p_x$ | 0.163 | 0.156 |
| C2, 3, 5, 6 | $2p_x$ | 0.092 | 0.066 |
|  | Σ | 1.000 | 1.016 |

## 6. The excited state spin-density distribution

In a semi-empirical analysis of hyperfine interaction constants one calculates a spin-density distribution rather than a wavefunction. Of course in the MO picture the wavefunction is spread out over the entire of the molecule (atoms and bonds) and the usage of atomic spin-densities can only be considered a first approximation. It is still very useful, especially when discussing chemical reactivity, to construct a picture of the spin-density distribution in a state.
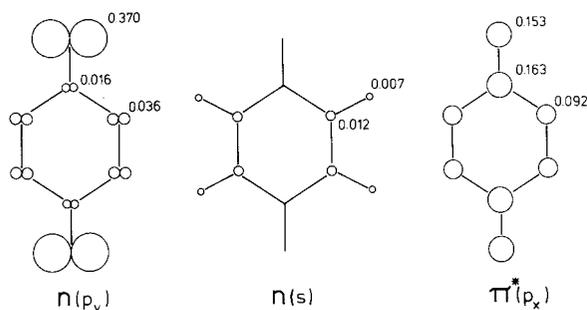


Fig. 2. The calculated gross atomic population (GAP) in the n and **p**\* orbitals of the lowest triplet state of *p*-benzoquinone. Note that the size of the orbital is chosen to be proportional to the square root of the GAP.

From the SCF wave function we can calculate what is known as the net atomic population (NAP) and the gross atomic population (GAP) [25] distribution. The NAP of an orbital at an atom is found by taking the square of the coefficient of this AO in the SCFMO. In the GAP the overlap contributions among different atoms are also taken into account. They are divided equally among the corresponding atoms and then added to the NAP. The GAP "spin-density distribution" should thus come closest to the spin-density distribution derived empirically. The semi-empirical calculations of the $2p_x$ and 2s spin-density at the non-carbonyl-carbon atom support this idea. Table 4 contains the net and gross atomic populations as calculated from the SCF triplet state wavefunction.

Note that the overlap corrections introduce appreciable shifts in the "spin-density distribution", which illustrates that an atomic spin-density distribution only gives a rough picture of the wavefunction. The GAP spin-density distribution in both the singly occupied n and **p**\* orbital is pictured in fig. 2. These pictures show that the unpaired **p**-electron is almost equally divided among the carbonyl groups and the central ringsystem. The unpaired n-electron density in contrast is largely confined (75%) to the oxygen atoms.

We further note that the **p**-electron spin-density distribution in the lowest triplet state of PBQ is very similar to the one determined for the *p*-benzo-semiquinone radical [26]. This confirms a previous assumption made [7] that the correlation effects between the n and **p**-electron are small. As this was also shown to be the case for the **p** and **p**\*-electron in the lowest triplet state of naphthalene [27] it does not seem to be farfetched to suggest that presumably in general for large molecules correlation effects between the unpaired electrons are small. This than seems a very useful *rule of thumb* in a semi-empirical analysis of the spin-density distribution in the lowest photo-excited triplet state of (hetero-) aromatics.

## 7. Summary and conclusions

This paper contains the results of an ab-initio calculation of the hyperfine coupling parameters in the lowest triplet state of *p*-benzoquinone.

A general conclusion is that interference effect contributions to the hyperfine splittings cannot always be

ignored. Analysis of the calculations further shows that only the oxygen hyperfine coupling parameters are completely determined by the **p** and n spin-density residing at oxygen and full determination of these parameters still remains desirable. The excellent agreement between the experiments and calculations leads us to the conclusion that the SCF description of the singly occupied orbitals is basically correct.

The conclusion then is that the unpaired **p**-electron is delocalized over the molecule, while the n-electron is largely confined to the oxygen atoms. The effect of the delocalization of the n-electron however is clearly recognizable and cannot be ignored in the analysis of the ENDOR data. In this regard we find it very surprising that Hutchison and Kohler [28] and Anderson and Kohler [29], in an analysis of the proton-ENDOR data of diphenylmethylene were able to consistently interpret their results by assuming that the **s** spin-density in this molecule is completely localized at the methylene carbon atom. This paper shows that in the case of PBQ such an assumption would have completely failed. The excited state electron spin-density distribution obtained for PBQ also justifies one of our previous assumptions [6] , namely that the contribution of the second-order spin-orbit coupling at oxygen completely dominates the fine-structure parameter of PBQ.

Finally the ab initio SCF wavefunctions used in this study should provide an excellent basis for vibronic coupling calculations [30] on the lowest triplet state of PBQ.

## References

[1] H.P. Trommsdorff, J. Chem. Phys. 56 (1972) 5358.
[2] R.L. Fulton and M. Gouterman, J. Chem. Phys. 41 (1964) 2280;
R.M. Hochrasser and C.A. Marzzacco, in: Molecular luminescence, ed. E.C. Lim (Benjamin, New York, 1969) p.631;

A.R. Gregory, W.H. Henneker, W. Siebrand and M.Z. Zgierski, J. Chem. Phys. 65 (1976) 2071.
[3] H. Veenvliet and D.A. Wiersma, Chem. Phys. 2 (1973) 69; Chem. Phys. Letters 22 (1973) 87.
[4] H.P. Trommsdorff, Chem. Phys. Letters 1 (1967) 214; H. Veenvliet and D.A. Wiersma, Chem. Phys. Letters 33 (1975) 305.
[5] A.I. Attia, B.H. Loo and A.H. Francis, Chem. Phys. Letters 22 (1973) 537.
[6] H. Veenvliet and D.A. Wiersma, Chem. Phys. 8 (1975) 432.
[7] J.H. Lichtenbelt, J.G.F.M. Fremeijer, H. Veenvliet and D.A. Wiersma, Chem. Phys. 10 (1975) 107.
[8] J.H. Lichtenbelt, J.G.F.M. Fremeijer and D.A. Wiersma, Chem. Phys. 18 (1976) 93.
[9] G.A. van der Velde, Thesis, University of Groningen (1974).
[10] J. Trotter, Acta Cryst. 13 (1960) 86.
[11] H.T. Jonkman, Thesis, University of Groningen (1975); H.T. Jonkman, G.A. van der Velde and W.C. Nieuwpoort, Quantum Chemistry The State of the Art, Proceedings of S.C.R. Atlas Symposium, Vol. 4 (1974) p. 245.
[12] E.D. Becker, H. Ziffer and E. Charney, Spectrochim. Acta 19 (1963) 1871.
[13] R. Willstätter and S. Dorogi, Ber. 42 (1939) 2147.
[14] H.M. McConnell and J. Strathdee, Mol. Phys. 2 (1959) 129.
[15] C.A. Hutchison Jr. and G.A. Pearson, J. Chem. Phys. 47 (1967) 520.
[16] F.C. Adam and S.I. Weissman, J. Am. Chem. Soc. 80 (1958) 2057.
[17] W.V. Smith, P.P. Sorokin, I.L. Gelles and G.J. Lasher, Phys. Rev. 115 (1959) 1546.
[18] M. Broze and Z. Luz, J. Chem. Phys. 51 (1969) 749.
[19] K. Scheffler and H.B. Stegmann, Elektronenspin Resonanz (Springer, Berlin, 1970) chs. C and D.
[20] J.R. Morton, Chem. Rev. 64 (1964) 453.
[21] N.B. Wong and J.H. Lunsford, J. Chem. Phys. 55 (1971) 3007.
[22] T. Cole, C. Helles and H.M. McConnell, Proc. Natl. Acad. Sci. US 45 (1959) 525.
[23] M. Karplus and G.K. Fraenkel, J. Chem. Phys. 35 (1961) 1312.
[24] S. Fraga and G. Malli, Many electron systems. Properties and interactions (Saunders, Philadelphia, 1968) pp. 8, 70.
[25] R.S. Mulliken, J. Chem. Phys. 23 (1955) 1833.
[26] J. Gendell, J.H. Freed and G.K. Fraenkel, J. Chem. Phys. 37 (1962) 2832;
M.R. Das and G.K. Fraenkel, J. Chem. Phys. 42 (1965) 1350.
[27] H. Hirota, C.A. Hutchison Jr. and P. Palmer, J. Chem. Phys. 40 (1964) 3717;
A.D. McLachan, Mol. Phys. 5 (1962) 51.
[28] C.A. Hutchison Jr. and B.E. Kohler, J. Chem. Phys. 51 (1969) 3327.
[29] J.M. Anderson and B.E. Kohler, J. Chem. Phys. 65 (1976) 2451.
[30] M.F. Merienne-Lafore and H.P. Trommsdorff, J. Chem. Phys. 64 (1976) 3791.
[31] J.H. Lichtenbelt, J.G.F.M. Fremeijer and D.A. Wiersma, to be published.